Journal of Intelligent Systems and Internet of Things
Vol. 18, No. 01, PP. 218-226, 2026
DOI: https://doi.org/10.54216/JISIoT.180116

Diverse Geographical Region Analysis Based on Deforestation Rate Using Remote Sensing Image and Machine Learning Techniques

Abhilash S. Nath[1,*], Manu Gupta[2], J. Sirisha Devi[3], A Babisha[4], D. Venkata Ravi Kumar[5], B. Rama Subba Reddy[6]

[1]Assistant Professor, Department of Artificial Intelligence and Data Science, St. Joseph's Institute of Technology, OMR, Chennai, India

[2]Associate Professor, Department of Electronics and Communication Engineering, Sreenidhi Institute of Science and Technology, Hyderabad, India

[3]Professor, Department of Computer Science and Engineering, Koneru Lakshmaiah Education Foundation, Bowrampet, Hyderabad 500043, Telangana, India

[4]Assistant Professor, Department of Artificial intelligence and Data Science, Panimalar Engineering College, Chennai, Tamilnadu, India

[5]Assistant Professor, Department of Computer Science and Engineering, Aditya University, Surampalem, India

[6]Professor, Department of CSE, Mohan Babu University, Tirupati, India

Emails: abhilashsathyanath2@gmail.com; Manugupta5416@gmail.com; Siri.cse21@gmail.com; babisha15@gmail.com; ravikumar.venkat@gmail.com; rsreddyphd@gmail.com

Abstract

With direct implications for the regional climate, biogeochemistry, hydrology, and biodiversity, land cover change has been identified as one of the top priorities for the development of sustainable management plans. Among the primary causes of global warming are deforestation and forest fragmentation, which have profound effects on biodiversity preservation and ecosystem functioning. Machine learning techniques, like those employed in computer vision, have become widely used, making it possible to segment satellite images semantically to distinguish between areas that are forested and those that are not. This study presents a novel method for segmenting and classifying UAV images to detect deforestation using machine-learning models. In this case, noise reduction as well as normalisation is applied to input, which consists of UAV-based forest region photos. Semantic U-convolutional regressive neural network combined with deep radial quantile temporal neural network was then used to segment and classify this image. The suggested model's simulation analysis is assessed based on several metrics, including F-1 score, normalized coefficient ratio, average precision, AUC, and detection accuracy. proposed method yielded 97% detection accuracy, 93% normalized coefficient ratio, 91% AUC, F-1 score of 94% and 95% AVERAGE PRECISION.

Received: February 07, 2025 Revised: May 25, 2025 Accepted: July 01, 2025

Keywords: Biodiversity; Deforestation rate; Machine learning model; Regressive neural network; Radial quantile temporal

1. Introduction

Deforestation is an international issue that has influenced a large number of forests worldwide. Unfortunately, it is quite challenging to monitor rate at which this is happening for Caribbean islands. Popular satellites like Sentinel and

Landsat do not cover the Caribbean islands because their primary survey regions are United States and European Union. As a result, Caribbean Islands are compelled to employ alternative methods—like the one outlined in [1]—to acquire data on deforestation, which can be laborious and difficult for the public to access. It may also become outdated, in which case newer satellite photos will need to be annotated. Therefore, developing a method for tracking deforestation is a helpful tool since it would enable smaller Caribbean islands to gauge the rate of deforestation. Computer vision is able to address a number of issues in field of remote sensing, from cloud detection to crop as well as soil segmentation. Nonetheless, a sizable dataset is easily accessible and available for many of these issues; however, because it might be expensive to get, this is not the case for Caribbean islands. Because they enable the identification of selective logging affects components in addition to providing better spatial resolutions for the databases, remote sensing techniques are regarded as an efficient as well as economical method for this investigation [2]. One of the valuable remote sensing data products for analyzing impacts of selective logging is high-resolution photographs generated by Unmanned Aerial Vehicles (UAVs). This method has advantages over conventional survey techniques. A digital surface and a digital terrain method can be produced by photogrammetrically processing the stereo pictures obtained by the optical sensor on board the UAV using 3D reconstruction software. Furthermore, UAVs might be useful for site assessment because of the region's tiny size, diffused dispersion, and restricted access to harvest places. A tree stump is one of the most significant as well as reliable signs in a selective logging area. Tree stumps in tropics are rather uniform and have a lighter color layer on their surface than those in their adjacent regions, which makes them harder to spot from a distance (10–50 cm) [3]. To identify stumps from high-resolution imaging, object-based image analysis (OBIA) as well as object detection-based techniques like template matching (TM) applied. The majority of TM algorithms' primary feature is object boundaries. But occasionally, the border can become distorted or blurry, making it difficult to determine the precise shape of the tree stump [4]. The problem of automated deforestation detection as well as mapping has seen a promising answer and substantial potential in recent years with advent of DL image segmentation techniques. These methods have demonstrated a great deal of promise in terms of improving efficiency as well as accuracy in identification and division of deforested regions. One kind of ML technique that can automatically categories each pixel in a picture according to its own distinct properties is called DL-based image segmentation. In deep learning-based image segmentation, a DNN is trained to automatically identify attributes of interest, allowing each pixel to be categorized into a distinct class. By massive satellite photo datasets for training deep learning models, these techniques are able to quickly and precisely detect deforested areas throughout the world. With the ability to precisely identify and map deforested regions, this method may improve forest management and monitoring. This makes it possible to precisely identify changes in the terrain, including shifts in the forest cover [5].

2. Research contribution

To suggest a unique method for segmenting and classifying machine learning models used in UAV image-based deforestation identification. Here, the input was gathered as UAV-based photos of the woodland region, and noise reduction and normalization were applied during processing. Next, a deep radial quantile temporal neural network combined with a semantic U-convolutional regressive neural network was used to segment and classify this image. The quality and accuracy of an image are directly correlated, and our experimental research demonstrates that image classification may be carried out in low-cost computing systems. The findings suggest that drones and other inexpensive computer resources can be used to monitor rainforests.

3. Literature review

One issue that is still very relevant today is the idea of adopting less powerful alternatives to deep learning techniques. This is because a lot of developing nations still have restricted access to devices like GPUs, which are more widely available in developed nations. Furthermore, several issues have restricted access to resources, necessitating the use of various features of the data that they are being applied to. Consider the issue of on-board semantic segmentation for aerial image processing in the context of UAVs. The drone's inbuilt technology restricts people from entering this area. They employed this notion to help identify photos on a farm, but they concentrate on difficulty of differentiating between crops, weeds, background. They did this by taking advantage of the fact that plants have a different NDVI that may be utilized to distinguish between soil and plants on a farm, done by [6]. YOLOV3 was proposed in work [7] to use unmanned aerial vehicle (UAV) photos to identify green mangoes in orchards. YOLO's drawback, however, is that it has trouble identifying small objects and produces more localization errors because each image grid can only suggest two bounding boxes. An object-based CNN has been proposed by author [8] to map and recognize seven different species of trees based on the forms and contrasts of their leaves. However, CNN's disadvantage is that it is very hard to distinguish between different species of trees with identical leaf patterns, and it requires large data sets to process multispectral and hyperspectral data, which lengthens the training process. Work [9] used airborne

hyperspectral data to categories various tree species, including birch, beech, larch, alder, and spruce, using SVM, random forest (RF), artificial neural networks (ANN). Author [10] suggested utilizing CNN and SVM, two classifiers, to distinguish between the leaf patterns of Flavia and Swedish plants. However, one of the SVM classifier's drawbacks is that selecting the SVM kernel and its hyperparameters for classification is a challenging operation. Using a pre-trained CNN and YOLOv2 method, method in [11] detected deciduous trees with an average precision of 67.3% and Cohune palm trees with an average precision of 79.5%. Author in [12] utilized Google's CNN Inception v3 with transfer learning as well as sliding windows to detect coconut trees with a precision of 71% and a recall 93%. Finally yet importantly, the method in [13] taught GoogLeNet method to classify seven distinct types of trees with an 89% accuracy rate by first segmenting aerial forest pictures into individual tree crowns utilizing eCognition tool. Notably, all of these techniques are trained to identify tree crowns that are visible in images; they do not, however, make an effort to distinguish or divide the tree crowns. Consequently, trained CNNs are unlikely to identify a tree crown that is mostly obscured by taller trees.

4. Proposed model in UAV image based deforestation detection utilizing ML model

In Fig. 1, the work flow diagram is displayed. The graph's water bodies are designated as vertices, and the weighted edges show how connected the vertices are to one another. The suggested runtime is O(n3). The suggested system makes decisions to contain the forest fire based on real-time data. Modern image processing algorithms make sure that any smoke or forest fire is identified right away, making them valuable for real-time applications.

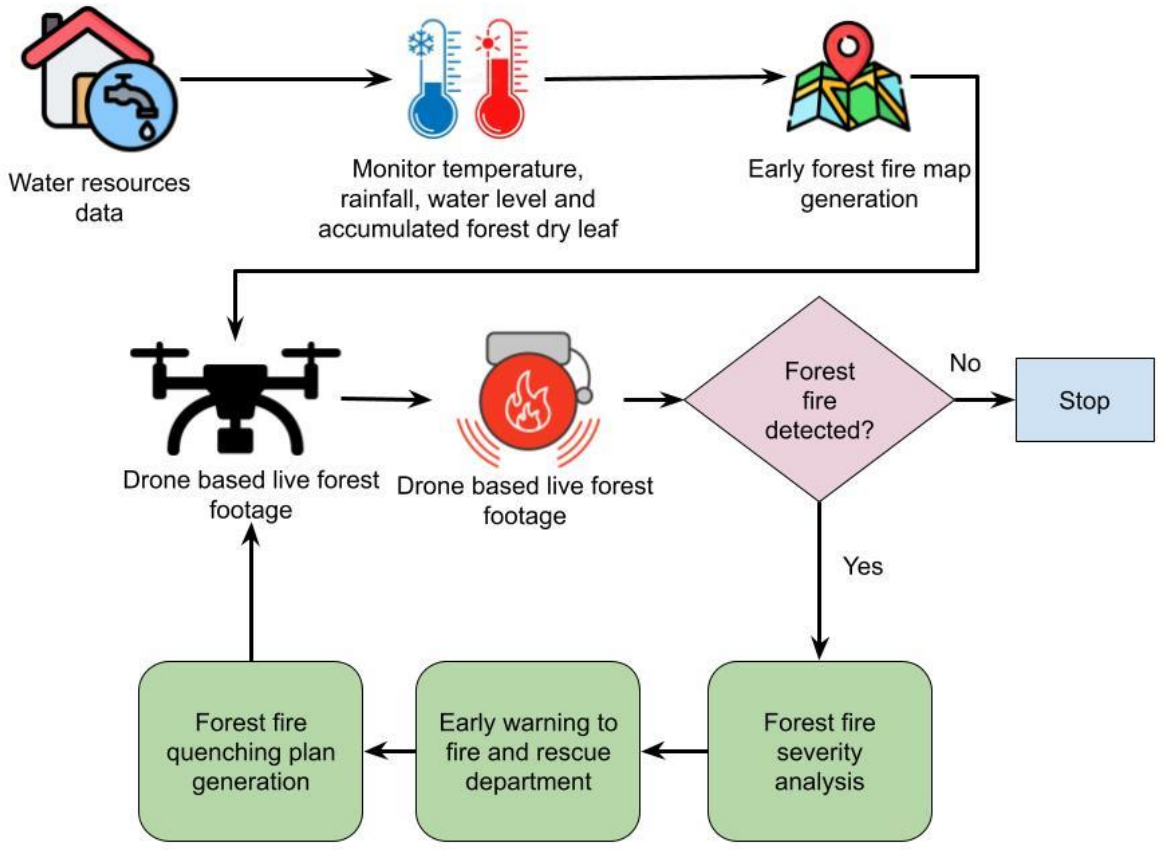

Figure 1. Work flow diagram for proposed model-based early forest deforestation detection

Drone Moment to the Target

(i) Throughout the entire operation, UAV navigation is crucial for patrolling regions that pose a risk or have experienced a fire. This work uses the navigational analysis technique to monitor the forest region. The drone performs the navigating to make this easier. The three navigational features of UAVs are as follows:

(ii) Awareness: This gives information about nearby impediments that a UAV may encounter. The internal sensors are used to gather the data.

(iii) Basic Navigation: Birds, trees, poles, and other objects in the forest farms are identified and avoided to prevent collisions. (iii) Expanded Navigation: This feature set includes advanced functions that are essential to autonomous navigation, like pathway planning and depth deployment.

To anticipate each bounding box, the network makes use of characteristics from the full image. Input image is divided into a S∗S grid, where S is set to 7. An object's center falls into a grid cell, and that grid cell is in charge of detecting it. There are two completely linked layers in the network after 24 convolutional layers. Our network ultimately yields S ∗S ∗31 tensor of predictions, with the third dimension calculated as follows: (5 predictions per bounding box) * (2 predictions per cell for bounding boxes) + (total classes). Each grid cell's 21 class probabilities are contained in the tensor. For every cell with probabilities higher than the threshold, we output the detection.

Dataset description: The UAVs-FFDB, or Unmanned Aerial Vehicles-based Forest Fire Database, is distinguished by its dual composition. First, it includes a set of 1653 high-resolution RGB raw photographs that were painstakingly taken using a normal S500 quadcopter frame and a RaspiCamV2 camera. Second, the database includes augmented data, resulting in 15560 photos overall, improving the dataset's diversity and comprehensiveness. In the wooded area next to Adana Alparslan Türkeş Science and Technology University in Adana, Turkey, these pictures were taken. The raw data subset of the dataset has a total size of 692 MB. The dimensions of each raw image in dataset range from 353 × 314 to 640 × 480, while the augmented data extends from 398 × 358 to 640 × 480. The augmented data subset, on the other hand, represents a much greater size, coming in at 6.76 GB. During a UAV surveillance operation, camera is properly tilted at -180 degrees to be horizontal to the ground, resulting in raw photos. To increase the diversity of field of view and create a more inclusive database, photographs are taken at intervals of 5 to 15 meters in altitude. The average UAV speed during the surveillance mission is 2 m/s.

Data from SiDroForest field in the summer of 2018, extensive expeditions from German Alfred Wegener Institute (AWI) Helmholtz Centre for Polar and Marine Research, in collaboration with North-Eastern Federal University of Yakutsk (NEFU). Bigger regions were separated into 12 subregions, which were called by closest city or lake to plots. For Chukotka, established 3 subregions that had 41 vegetation plots, for central Yakutia, designated 9 subregions that included 23 vegetation plots. The tree cover varies among the vegetation plots; on slopes and in lowlands, it ranges from treeless tundra to open larch forests, with the density of trees varying according to slope aspect. This dataset's data kinds are connected to one another by means of a two-letter code that represents the vegetation plot numbers and the subregion.

UAVS-FDDB: UAV-based Database for Forest Fire Detection - In the wooded areas surrounding Adana Alparslan Türkeş Science and Technology University, Adana, Turkey, the photographs were taken with unmanned aerial vehicles (UAVs) fitted with Raspberry Pi Camera V2 technology. This dataset consists of two primary parts, each with an annotation file: the original (raw) data and the augmented data. There are 1,653 photos in the raw data and 15,560 images in the augmented dataset. The distribution of images among the four classes is shown below - Unprocessed Information Forest Condition Prior to Evening = 222 Condition of the Evening Forest = 286 791 is the pre-evening fire incident; 354 is the nighttime fire incident.

5. Semantic U-convolutional regressive neural network with deep radial quantile temporal neural network (SU-CRNN-DRQTNN)

The convolution and deconvolution networks make up the two components of our trained network. While deconvolution network is a shape generator that creates object segmentation using the feature retrieved from convolution network. It is evident that the propagation in the deconvolutional layers reconstructs coarse-to-fine object structures; higher layers typically uncover more intricate patterns, while lower layers typically record an object's general coarse configuration (e.g., position, form, and region). Keep in mind that the roles that unpooling and deconvolution play in the creation of segmentation masks differ. By returning to image space, the original places with strong activations, unpooling captures example-specific structures. It successfully recreates an object's intricate structure at higher resolutions as a result. On the other hand, learnt filters in deconvolutional layers typically capture class-specific shapes. Deconvolutions efficiently decrease noisy activations from other regions while amplifying the activations closely connected to the target classes. With unpooling and deconvolution combined, our network produces precise segmentation maps.

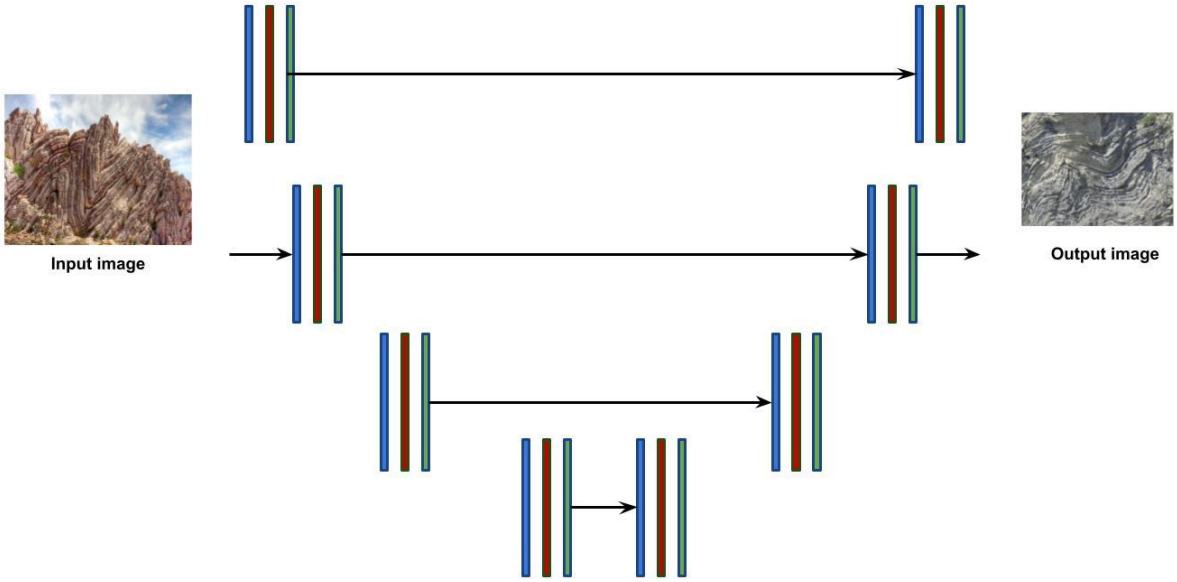

Figure 2. U-net Convolutional model

Similar to semantic segmentation approach and a completely CNN technique, U-Net uses a fully convolutional network to achieve semantic segmentation. With an encoder that finds spatial information in image and a decoder that uses those features to create a segmentation map, network is designed to be symmetrical. After each downsampling, this process is repeated four times, increasing number of convolution layer filters by one. Two 3x3 convolutional procedures are used to link the encoder and decoder. Conversely, the decoder first uses a 2×2 transposed convolutional operation to up sample the feature map, which reduces the number of feature channels by half. A series of two 3x3 convolutional processes come after this. The four iterations of this upsampling and two-convolutional processing cycle involve halving number of filters in each cycle to align with the encoder. The 1×1 convolutional method is used to generate the final segmentation map. All layers use Rectified Linear Unit (ReLU) activation function; final convolutional layer uses sigmoid activation function. Usage of skip connections is one of most unique aspects of U-Net architecture. Before encoder is pooling operation, convolutional layer's output is transferred to the matching layer in the decoder. The architecture of U-Net is shown in Figure 2, which includes skip connections between relevant layers in both encoding as well as decoding paths.

The RBF network is a feedforward neural network with three layers (J1-J2-J3). Nonlinear activation function of every node in hidden layer is a radial basis function (RBF), given by symbol υ(r). The hidden layer nonlinearly transforms input layer, and the nonlinearity is mapped into a new space by a linear combiner in the output layer. By applying the linear optimization method, RBF network finds a globally optimal solution to changeable weights in sense of minimum mean square error (MSE). RBF network's output for an input is provided by eqn (1)

$$y_i(\vec{x}) = \sum_{k=1}^{J_2} w_{ki}\phi(\|\vec{x} - \vec{c}_k\|),\ i = 1, \dots, J_3 \qquad (1)$$

For a set of *N* pattern pairs $\{(\vec{x}_p, \vec{y}_p) \mid p = 1, \dots, N\}$, is given in matrix form is given by eqn (2)

$$\mathbf{Y} = \mathbf{W}^T\mathbf{\Phi} \qquad \mathbf{(2)}$$

A receptive-field or localized network is an RBF network with a localized RBF, such as Gaussian RBF network. The best results are obtained from the localized approximation method when the input is close to a node's prototype. Nearby input vectors always, create identical outputs for a well-trained localized RBF network, but distant input vectors yield outputs that are almost independently generated. The intrinsic quality of local generalization is this. Similar to an associative neural network, a receptive-field network determines only a limited subspace based on its input. This trait is especially appealing since it results in a local effect when receptive-field function is modified. Therefore, by modifying the receptive-field functions' parameters and/or adding or removing neurons, receptive-field networks can be easily built.

The complexity of the hθ estimator must grow correctly and quickly as sample size increases. NN sieve's structure is as follows: t = 1, 2, ⋯, n is given by eqn (3)

$$Y_t = h_\theta(X_t) + \varepsilon_t = \sum_{m=1}^{M_n} w_m^o \psi\left(\sum_{k=1}^{K} w_{k,m}^h X_{k,t} + b_m^h\right) + b_o + \varepsilon_t \quad (3)$$

Two categories of parameters exist: parameters for hidden layer (wh k, m, bh m) and parameters for the output layer. It is simple to extend to a quantile regression context. Examine linear quantile regression formula presented in Koenker and Bassett for a fixed quantile level τ is given by eqn (4)

$$Y_t = X_t\beta + \varepsilon_t,\ t = 1, \dots, n \quad (4)$$

assuming Qτ (εt|Xt) = 0. Dependent variable Yt is represented in this context as a linear function of the independent variables Xt. Following minimization issue can therefore be solved using the linear quantile estimator is given by eqn (5)

$$\min_\beta \sum_{t=1}^{n} \rho_\tau(Y_t - X_t\beta) \quad (5)$$

where |z|·|τ − I(z < 0)| = ρτ (z) is loss function for quantiles. Simplex or interior point methods can be utilized to tackle this less issue since it is expressed as a linear program. A nonlinear extension of this regression paradigm is NN quantile regression. NN sieve estimator is used to approximate the conditional quantile instead of a linear function. Resulting optimization issue is nonconvex, meaning that linear programming techniques are inapplicable is given by eqn (6)

$$\min_\theta \sum_{t=1}^{n} \rho_\tau\{Y_t - h_\theta(X_t)\} \quad (6)$$

Neural networks' large capacity makes them vulnerable to overfitting. The selection of the neural network's hyperparameters and structure provides an efficient means of preventing overfitting. Number of hidden nodes, Mn, is the most crucial hyperparameter in our single hidden layer setup. Learning algorithm's definition and the quantity of epochs are further essential parameters. Hyperparameters are typically chosen using a cross-validation criterion. Adding an additional penalty term to weight parameters, wh k, m, wo m, provides an alternative strategy.

6. Results and discussion

Experimental setup- Experiments are carried out using Colab on Core-I3 systems with 13GB of RAM from Google Colab Laboratory and 8GB on the PC. For testing, the 4 CPU's 1.7 GHz processor is used. The data set is composed of three parts: the detection set, the cross-validation set, and the testing set. K-Fold Cross-validation was used. 70% of the dataset is used as a detection set, and the remaining 30% is used for testing. Cross validation is used for both the testing and detection sets.

7. Comparison results based on UAV image based deforestation detection

Table 1: Comparative analysis between proposed and existing technique for UAV image based deforestation dataset

Dataset	Techniques	Detection accuracy	Average precision	Normalized coefficient ratio	AUC	F-1 score
UAVS-FFDB	GLCM	71	69	72	77	70
	SEGNET	76	77	78	82	75
	SU-CRNN-DRQTNN	81	84	82	86	83
SIDROFOREST	GLCM	75	77	79	78	68
	SEGNET	80	84	83	81	72
	SU-CRNN-DRQTNN	83	89	91	90	82

UAVS-FDDB	**GLCM**	74	70	76	81	78
	SEGNET	84	85	89	87	90
	SU-CRNN-DRQTNN	97	95	93	91	94

Table 1 above shows a comparison of the proposed and existing methods for several UAV image-based deforestation datasets. Here, multi-modal watermarked picture datasets from UAVS-FFDB, SIDROFOREST, and UAVS-FDDB are used to analyse the proposed approach. Study conducted a parametric analysis focusing on detection accuracy, normalized coefficient ratio, AUC, F-1 score and average precision.

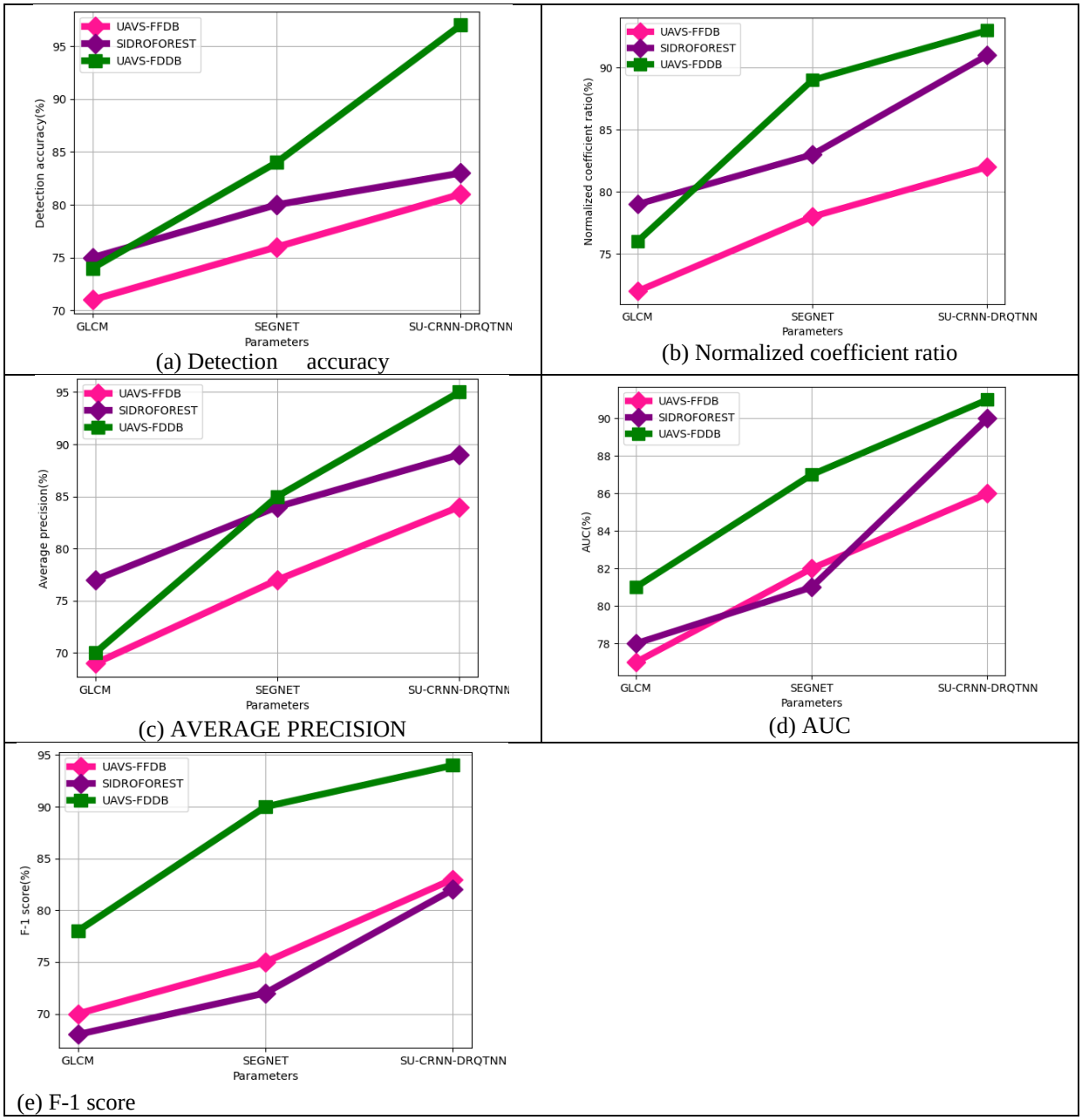

(a) Detection accuracy

(b) Normalized coefficient ratio

(c) AVERAGE PRECISION

(d) AUC

(e) F-1 score

Figure 3. Comparative analysis for Financial data based socio economy analysis in agriculture dataset in terms of (a) Detection accuracy, (b) Normalized coefficient ratio, (c) AVERAGE PRECISION, (d) AUC, (e) F-1 score

Figure 3(a)–(d) compares the suggested and existing methods for financial databased socioeconomic analysis in the agriculture dataset. Recommended method in this instance produced detection accuracy of 81%, normalized coefficient ratio of 82%, AUC of 86%, F-1 score of 83% and average precision of 84%. For the UAVS-FFDB dataset, SEGNET achieved 71% detection accuracy, 72% normalized coefficient ratio, 77% AUC, F-1 score of 70% and 69% AVERAGE PRECISION, in contrast to the prior GLCM, which achieved 76% detection accuracy, 78% normalized coefficient ratio, 82% AUC, F-1 score of 75% and 77% AVERAGE PRECISION. 83% detection accuracy, 91% normalized coefficient ratio, 90% AUC, F-1 score of 82% and 89% average precision were outcomes of recommended method. SEGNET obtained 80% detection accuracy, 83% normalized coefficient ratio, 81% AUC, F-1 score of 72% and 84% average precision on SIDROFOREST dataset. With detection accuracy 75%, normalized coefficient ratio 79%, AUC 78%, F-1 score 68% and average precision 77%, GLCM performed well. For UAVS-FDDB dataset, recommended method yielded 97% detection accuracy, 93% normalized coefficient ratio, 91% AUC, F-1 score of 94% and 95% AVERAGE PRECISION. The SEGNET obtained 84% detection accuracy, 89% normalized coefficient ratio, 87% AUC, F-1 score of 90% and 85% AVERAGE PRECISION, while the current GLCM earned 74% detection accuracy, 76% normalized coefficient ratio, 81% AUC, F-1 score of 78% and 70% AVERAGE PRECISION. e, the underlying classifier, identifies regions that have probably seen deforestation. After that, the photo is visually analysed by a photointerpreter, or an inspector may be dispatched to the designated locations to determine which areas actually show deforestation and which merely false alarms are. This scheme's primary advantage is that human labour is limited to a specific area under observation. However, with this system, some of the deforested areas may go undiscovered since the classifier may miss them. In this investigation, the percentage of the monitored region marked as possibly deforested and the percentage of overall deforestation concentrated in the places the classifier identified are the two most important measures. Unichannel 2D images are created by casting onboard infrared sensors to determine the forest farm's heat distribution. The temperature of the forest fire determines its classification into three zones, which may be identified from the UAV using very precise infrared sensors that assess the intensity of forest fire pixels and determine which category they come under. A graph is created using the pixel brightness, and the high-intensity zone is defined as the local maxima.

8. Conclusion

Deep learning-based algorithms are very useful methods since they have demonstrated good results in the classification of remote sensing pictures. In this study, we used a supervised image classification method based on DL and UAV photos to classify forest areas. This study offers a novel approach to detect deforestation by utilizing machine learning algorithms to segment and classify UAV photos. Here, normalization and noise reduction procedures were applied to UAV-based forest region images that were utilized as input. This image was then segmented and classified using a deep radial quantile temporal neural network and a semantic U-convolutional regressive neural network. Our test results show that the DL strategy provides better accuracy when compared to other ML methods. Cross-validation showed that the overall accuracy of the deep learning method is around 97%. This work highlights how important it is to combine UAV observations and deep learning in the planning and management of forest zones, which are often endangered by deforestation and encroachment.

References

[1] J. V. Solórzano, J. F. Mas, J. A. Gallardo-Cruz, Y. Gao, and A. F. M. de Oca, "Deforestation detection using a spatio-temporal deep learning approach with synthetic aperture radar and multispectral images," *ISPRS J. Photogramm. Remote Sens.*, vol. 199, pp. 87–101, 2023.

[2] Y. C. Putra and A. W. Wijayanto, "Automatic detection and counting of oil palm trees using remote sensing and object-based deep learning," *Remote Sens. Appl.: Soc. Environ.*, vol. 29, p. 100914, 2023.

[3] B. Haq *et al.*, "Tech-Driven Forest Conservation: Combating Deforestation With Internet of Things, Artificial Intelligence, and Remote Sensing," *IEEE Internet Things J.*, 2024.

[4] R. D. D. Altarez, A. Apan, and T. Maraseni, "Deep learning U-Net classification of Sentinel-1 and 2 fusions effectively demarcates tropical montane forest's deforestation," *Remote Sens. Appl.: Soc. Environ.*, vol. 29, p. 100887, 2023.

[5] A. Buchelt *et al.*, "Exploring artificial intelligence for applications of drones in forest ecology and management," *For. Ecol. Manage.*, vol. 551, p. 121530, 2024.

[6] S. Srivastava and T. Ahmed, "DLCD: Deep learning-based change detection approach to monitor deforestation," *Signal, Image Video Process.*, pp. 1–15, 2024.

[7] T. A. T. Do, H. D. Tran, and A. N. T. Do, "Classifying forest cover and mapping forest fire susceptibility in Dak Nong province, Vietnam utilizing remote sensing and machine learning," *Ecol. Inform.*, vol. 79, p. 102392, 2024.

[8] V. Nasiri, P. Hawryło, P. Janiec, and J. Socha, "Comparing Object-Based and Pixel-Based Machine Learning Models for Tree-Cutting Detection with PlanetScope Satellite Images: Exploring Model Generalization," *Int. J. Appl. Earth Obs. Geoinf.*, vol. 125, p. 103555, 2023.

[9] Q. Wang, B. Tang, K. Wang, J. Shi, and M. Li, "Evaluation of the gully erosion susceptibility by using UAV and hybrid models based on machine learning," *Soil Tillage Res.*, vol. 244, p. 106218, 2024.

[10] A. R. Malipatil, C. V. Pallavi, and L. S. Geetha, "Investigation and Monitoring Deforestation by Evaluating the Satellite Images and Machine Learning," in *Proc. Int. Conf. Adv. Comput., Commun. Appl. Inform. (ACCAI)*, 2023, pp. 1–8.

[11] D. A. Subhahan and C. V. Kumar, "Deforestation rate estimation using crossbreed multilayer convolutional neural networks," *Multimedia Tools Appl.*, pp. 1–27, 2024.

[12] T. F. Olivatto, F. F. Inguaggiato, and F. N. Stanganini, "Urban mapping and impacts assessment in a Brazilian irregular settlement using UAV-based imaging," *Remote Sens. Appl.: Soc. Environ.*, vol. 29, p. 100911, 2023.

[13] O. W. Kent, T. W. Chun, T. L. Choo, and L. W. Kin, "Early symptom detection of basal stem rot disease in oil palm trees using a deep learning approach on UAV images," *Comput. Electron. Agric.*, vol. 213, p. 108192, 2023.